Estimation of rotor aerodynamics using blade element theory

Andra-Ana-Maria GHEORGHIU*[,1], Ionut BUNESCU[1,2],
Mihai-Vladut HOTHAZIE[1,2], Mara-Florina NEGOITA[1,2], Mihai-Victor PRICOP[1,2]

*Corresponding author
[1]INCAS – National Institute for Aerospace Research "Elie Carafoli",
B-dul Iuliu Maniu 220, Bucharest 061126, Romania,
gheorghiu.andra@incas.ro*, bunescu.ionut@incas.ro, hothazie.mihai@incas.ro,
negoita.mara@incas.ro, pricop.victor@incas.ro
[2]Department of Aerospace Sciences,
National University of Science and Technology POLITEHNICA Bucharest,
Gheorghe Polizu 1, 011061, Bucharest, Romania

DOI: 10.13111/2066-8201.2026.18.1.3

Received: 01 February 2026/ Accepted: 08 March 2026/ Published: March 2026

Abstract: *This paper presents a detailed analysis of the Blade Element Theory (BET) as applied to the aerodynamic performance of propellers and rotor systems. BET, a low-fidelity but widely used method, models the rotor blade as a series of independent elements along its span, allowing local aerodynamic forces to be calculated based on flow conditions. The approach combines the Blade Element Theory with Momentum Theory, implemented in a MATLAB program for a forward flight helicopter, facilitating the computation of thrust, torque and power coefficients. To account for inflow distribution and induced velocity effects, actuator disk theory is applied at the rotor disk level, providing a consistent estimation of the induced velocity required for accurate flow velocity values. The rotor solidity is used to compare lifting rotor system to an ideal actuator disk. Results demonstrate that the coupled method of BET and Momentum Theory provides accurate and consistent aerodynamic predictions for use in rotor design, optimization and validation against experimental measurements or CFD simulations.*

Key Words: *blade element method, helicopter, rotor aerodynamics, rotor induced velocity*

1. INTRODUCTION

The accurate estimation of rotor aerodynamics is essential for the design and performance analysis of rotary-wing aircraft, wind turbines, and propellers. Due to rotor blades limited capacity to transmit bending moments, a coning angle of 5°, is required to transfer lift forces to the rotor hub via blade tension. These aerodynamic lift forces, which must support the aircraft's gross weight, are generated by blades comprising less than 5% of that weight, yet subjected to centrifugal forces several times greater. While stationary rotor blades can be easily damaged, they become rigid once spinning [1].

One of the foundational contributions to the development of Blade Element Theory (BET) is presented in [2]. However, the formulation presented in this work neglects the effects of induced flow within the propeller stream tube [3]. As the velocity of the airflow within the stream tube exceeds that of the undisturbed far-field, this omission results in an altered angle of attack on the blade elements, thereby introducing discrepancies in thrust prediction. The method was further improved through the incorporation of the Rankine–Froude momentum theorem, also known as actuator disk theory, leading to the formulation of Blade Element Momentum Theory (BEM) [4]. This combined approach enables the determination of the induced velocity and the corresponding induced angle-of-attack distribution along the blade. The BET was developed to include the influence of the vortical wake through an induced angle of attack component as calculated by Biot-Savard law [5].

Blade Element Theory applies conventional airfoil theory to rotating blades. Although rotor blades are structurally flexible, they are typically assumed to be rigid. This assumption is justified by the dominance of centrifugal forces, which maintain the blade in an effectively rigid configuration during normal rotation speeds [6]. Blade Element Theory offers a modelling approach that enables the detailed estimation of aerodynamic forces and moments acting on individual segments of a rotor blade. This is achieved by conceptualizing the blade as being divided into a series of narrow, chordwise-oriented strips or elements, each treated as aerodynamically independent from the others. A precise determination of the aerodynamic coefficients at various blade stations is essential for the accurate and effective application of the blade element method [7].

Among the various analytical approaches, Blade Element Theory (BET) remains one of the most widely used due to its simplicity, flexibility, and ability to provide meaningful insights into rotor behavior with relatively low computational cost. It is the foundation of almost all analyses of helicopter aerodynamics, dealing with detailed flow and loading of the blade and thus, relates the rotor performance and other characteristics to the detailed design parameters. The Momentum Theory is a global analysis, which along with Blade Element Theory provides useful results for the rotor design [8].

This study presents a comprehensive application of Blade Element Theory to estimate rotor aerodynamic performance. The methodology serves as a foundational tool for both preliminary design and performance validation of rotating wing systems by illustrating a helicopter rotor divided into a number of elements. It highlights the initial data used to locate the blade and the impact of various parameters on thrust and power output. The obtained results of a helicopter rotor in a MATLAB program based on Blade Element Theory are indicated and evaluated.

2. MATHEMATICAL MODELLING

Although CFD enables detailed analysis and accurate prediction of aerodynamic interference effects at the preliminary or detailed design stage, low-fidelity methods are generally preferred for parametric studies and design space exploration during the initial sizing or conceptual design stage [9]. The Blade Element Theory offers numerous advantages for the estimation of rotor aerodynamics. It allows the inclusion of variations in airfoil geometry, chord length, and pitch angle along the blade span, resulting in a more accurate representation of the propeller's aerodynamic performance. It estimates propeller thrust by dividing each blade into multiple segments, known as blade elements, and treating each as an independent two-dimensional airfoil [4]. This approach facilitates the evaluation of the aerodynamic forces based on the local flow conditions at each element. Once the forces on all elements are determined, they are integrated to obtain the overall thrust and torque of the propeller and then the corresponding power can be calculated.

Distinct from the Momentum Theory, the BET can be used to design the rotor blades of a helicopter in terms of blade twist, planform distribution and airfoil shape, to provide a given general rotor performance [5].

The actuator disk theory is a mathematical model used to describe idealized actuator disks, commonly applied to helicopter rotors. In this model, the rotor is represented as an infinitely thin disk that produces a uniform velocity along its axis of rotation. The disk generates a flow around the rotor, enabling the derivation of mathematical relationships between power, rotor radius, induced velocity, torque and thrust [10].

A rotor of radius R rotating with an angular velocity of Ω $[rad/s]$, divided into a finite number of discrete sections was analysed. Fig. 1 shows a representative blade element, where $c(r)$ is the chord length and dr is the infinitesimal width. The element is positioned at a radial distance, r, from the centre of rotation [4].

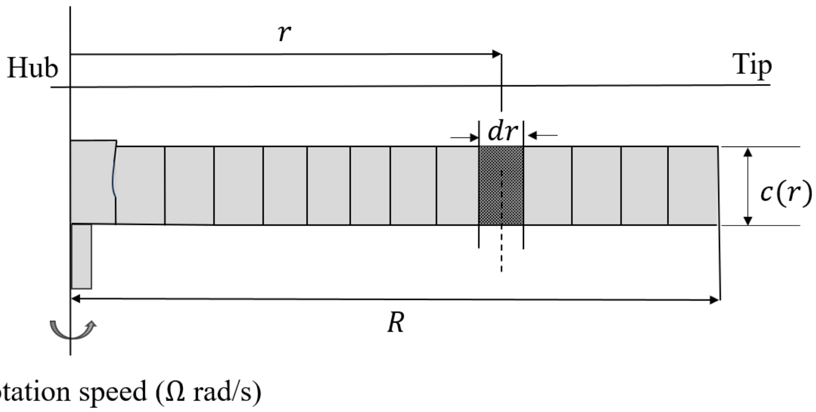

Fig. 1 Blade element subdivisions

A cross-sectional view of the blade element is shown in Fig. 2, illustrating the components of the local airspeed and the associated flow angles. This includes the axial and tangential velocity components, the resulting relative airflow and the corresponding geometric and aerodynamic angles [4]:

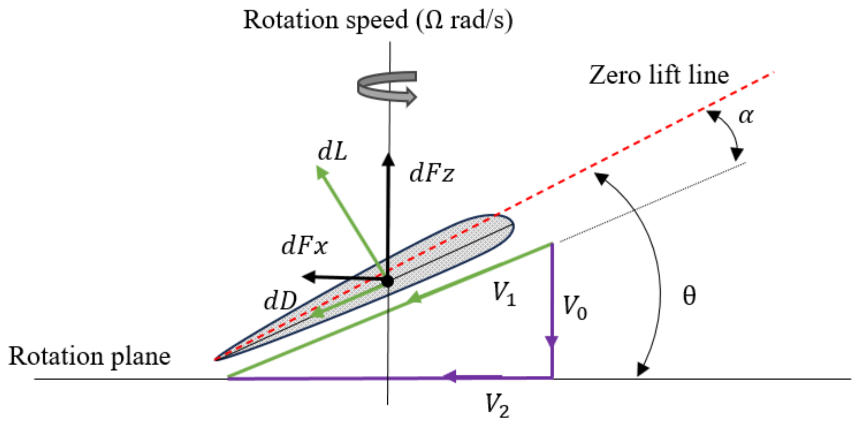

Fig. 2 Flow on the blade

where V_0 is the axial flow velocity vector at rotor disk, V_2 is the tangential flow velocity vector and V_1 is the section local flow velocity vector, summation of vectors V_0 and V_2.

It is necessary to fix parameters such as the blade element radius, the cartesian coordinates of the rotor, the azimuth angle and the radial position along the radius in order to locate the blade element selected for analysis. Thus the radius element is:

$$dr = \frac{R_B - R_0}{n_R - 1} \tag{1}$$

where R_0 represents the hub radius, R_B is the rotor radius and n_R denotes the number of radial elements (divisions along the blade span).

The azimuth angle ψ_i is defined based on the number of azimuthal steps n_ψ (positions around the rotor disk):

$$\psi_i = (i-1)\frac{360}{n_\psi - 1}, where\ i = 1 \div n_\psi \tag{2}$$

The azimuth angle is a key parameter in understanding rotorcraft aerodynamics, as it describes the position of a blade element during its rotation. The radial position along the radius is:

$$R_j = R_0 + (j-1)\frac{R_B - R_0}{n_R - 1}, where\ j = 1 \div n_R \tag{3}$$

The rotor cartesian coordinates can be defined as:

$$\begin{cases} x_{i,j} = R_j \cos\left(\psi_i \frac{\pi}{180}\right) \\ y_{i,j} = R_j \sin\left(\psi_i \frac{\pi}{180}\right) \end{cases} \tag{4}$$

Fig. 3 presents the top view of the rotor, highlighting the azimuth angle and the blade element positioning:

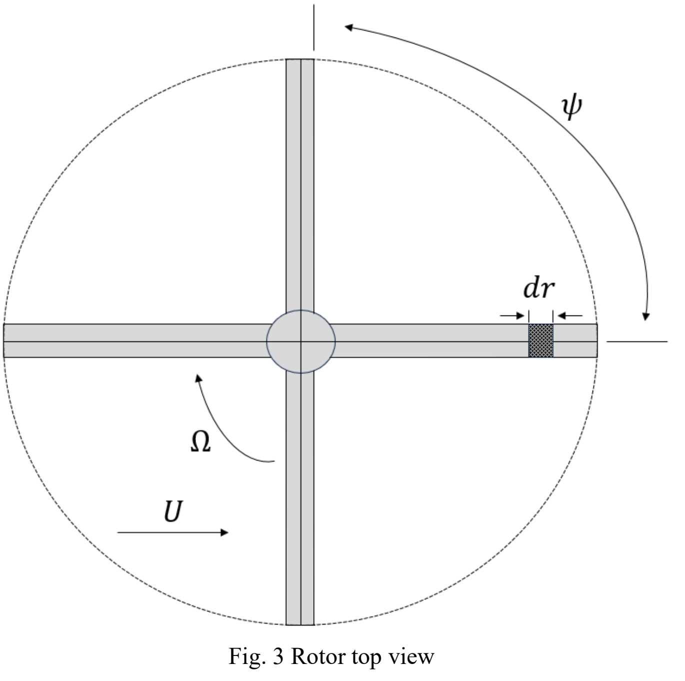

Fig. 3 Rotor top view

The blade twist angle is:

$$\theta_{i,j} = \theta_0 - \theta_{tw} R_j \tag{5}$$

where θ_0 is the blade torsion at hub and θ_{tw} represents the blade torsion rate. Fig. 4 presents the helicopter side view in forward flight, illustrating the helicopter angle of incidence:

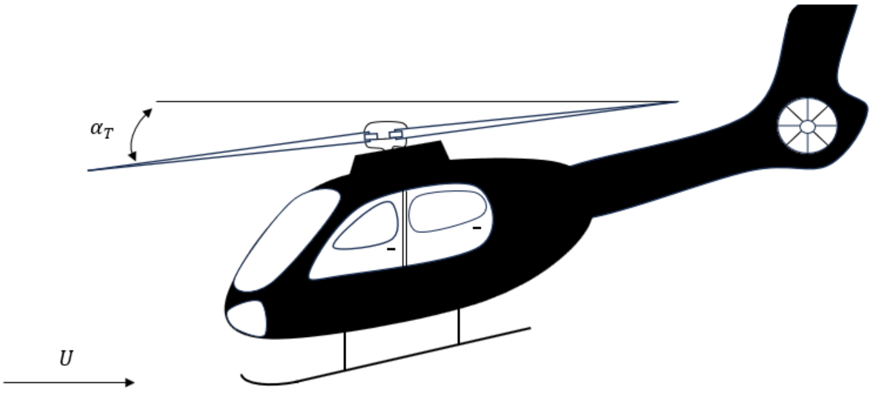

Fig. 4 Helicopter side view in forward flight

The flow around the rotating blade needs to be analyzed for the performance and efficiency of the helicopter rotor. The normal flow velocity component is perpendicular to the rotor disk and it is:

$$V_{0_{i,j}} = V_{I_{i,j}} + V_C + U \sin\left(\alpha_T \frac{\pi}{180}\right) \tag{6}$$

where $V_{I_{i,j}}$ is the induced velocity, V_C is the helicopter climb velocity, U represents the helicopter cruise velocity and α_T indicates the helicopter angle of incidence.

The tangential flow velocity component is generated by the blade's rotation around the hub and it is defined as:

$$V_{2_{i,j}} = N_R \frac{2\pi}{60} R_j + U \cos\left(\alpha_T \frac{\pi}{180}\right) \sin\left(\psi_i \frac{\pi}{180}\right) \tag{7}$$

where N_R is the rotational speed of the rotor.

The resultant flow velocity is then obtained:

$$V_{1_{i,j}} = \sqrt{V_{0_{i,j}}^2 + V_{2_{i,j}}^2} \tag{8}$$

$V_{1_{i,j}}$ is used to calculate the aerodynamic forces acting on the element [4].

The flow angle relative to the rotor plane is:

$$\varphi_{i,j} = \tan^{-1}\left(\frac{V_{0_{i,j}}}{V_{2_{i,j}}}\right)\frac{180}{\pi} \tag{9}$$

The pitch angle of the blade is:

$$\beta_{i,j} = A \cos\left(\psi_i \frac{\pi}{180}\right) + B \sin\left(\psi_i \frac{\pi}{180}\right) + C \tag{10}$$

where A is the longitudinal cyclic pitch, B is the lateral cyclic pitch, C is the collective pitch.

The incidence angle of the flow is then calculated:

$$\alpha_{i,j} = \beta_{i,j} + \theta_{i,j} - \varphi_{i,j} \tag{11}$$

The elemental lift is:

$$dL_{i,j} = \frac{1}{2}\rho V_{1_{i,j}}^2 C_B d_R \left(C_{L0} + C_L^{\alpha}\alpha_{i,j}\right) \tag{12}$$

where ρ is the air density, C_B denotes the mean blade chord, and the lift coefficient is modeled using a linear relation, with C_{L0} representing the lift coefficient at zero angle of attack and C_L^{α} the lift slope, both characteristics of the airfoil employed.

The elemental drag is:

$$dD_{i,j} = \frac{1}{2}\rho V_{1_{i,j}}^2 C_B d_R \left[C_{D0} + \frac{1}{\pi\lambda e}\left(C_{L0} + C_L^{\alpha}\alpha_{i,j}\right)^2\right] \tag{13}$$

where C_{D0} is the drag coefficient at zero incidence, λ represents the blade aspect ratio, and e is the Oswald factor, typically between 0.8 and 0.9.

The elemental lift and drag are perpendicular and parallel to the resultant flow velocity, independently [5].

The elemental thrust is found by separating the lift and drag forces into components along the rotor axis, based on the local flow angle:

$$dT_{i,j} = dL_{i,j}\cos\left(\varphi_{i,j}\frac{\pi}{180}\right) - dD_{i,j}\sin\left(\varphi_{i,j}\frac{\pi}{180}\right) \tag{14}$$

The elemental torque is:

$$dQ_{i,j} = R_j\left[-dL_{i,j}\sin\left(\varphi_{i,j}\frac{\pi}{180}\right) + dD_{i,j}\cos\left(\varphi_{i,j}\frac{\pi}{180}\right)\right] \tag{15}$$

The elemental power represents the power applied to each blade element required to move it through air with torque:

$$dP_{i,j} = N_R\frac{2\pi}{60}dQ_{i,j} \tag{16}$$

The ideal induced velocity in the rotor calculated based on the actuator disk theory is:

$$V_{I_{i,j}}{}^{*} = \frac{dT_{i,j}}{4\pi\rho R_j V_{0_{i,j}} d_R} \tag{17}$$

First, to initiate the rotor aerodynamics computation, the induced velocity is initialized to a small value and the iteratively corrected using relation (17).

To prevent instability in the induced velocity solution, a Crank-Nicolson scheme is adopted, as shown in (18), in which the updated induced velocity is obtained as a weighted combination of the previous value and the newly computed value. This recursive procedure is repeated until the difference between two successive iterations falls below a prescribed convergence threshold.

$$V_{I_{i,j}} = 0{,}9\overline{V_{I_{i,j}}} + 0{,}1V_{I_{i,j}}{}^{*} \tag{18}$$

Once the aerodynamic forces are determined, they can be summed to determine the properties on the complete rotor.

Therefore, the thrust per azimuth is:

$$T_i = \sum_{j=1}^{n_R} dT_{i,j} \tag{19}$$

The resistive torque per azimuth is:

$$Q_i = \sum_{j=1}^{n_R} dQ_{i,j} \tag{20}$$

The required power per azimuth is:

$$P_i = \sum_{j=1}^{n_R} dP_{i,j} \tag{21}$$

To determine the thrust coefficient, as well as the resistive torque and power, the average values of thrust, torque, and power must first be calculated. Accordingly, the average thrust is defined as:

$$T_m = \sigma \sum_{i=1}^{n_\psi} T_i \tag{22}$$

where

$$\sigma = \frac{N_B \cdot C_B (R_B - R_0)}{\pi (R_B - R_0)^2} \tag{23}$$

represents the rotor solidity.

The average resistive torque is obtained from the resistive torque per azimuth:

$$Q_m = \sigma \sum_{i=1}^{n_\psi} Q_i \tag{24}$$

The average required power is obtained from the required power per azimuth:

$$P_m = \sigma \sum_{i=1}^{n_\psi} P_i \tag{25}$$

The thrust coefficient is:

$$C_T = \frac{T_m}{\frac{1}{2} \rho \left(\frac{N_R}{60} R_B \right)^2 N_B \cdot C_B (R_B - R_0)} \tag{26}$$

where N_B represents the number of blades.

The resistive torque coefficient is:

$$C_Q = \frac{Q_m}{\frac{1}{2} \rho \left(\frac{N_R}{60} R_B \right)^2 R_B N_B C_B (R_B - R_0)} \tag{27}$$

The power coefficient is:

$$C_P = \frac{P_m}{\frac{1}{2}\rho\left(\frac{N_R}{60}R_B\right)^3 N_B C_B (R_B - R_0)} \tag{28}$$

The sectional lift coefficient at the tip of a lifting surface tends to zero due to tip effects. Similarly, at the hub, the lift coefficient decreases to zero as the radial position approaches the root. The BET analysis ignores this effect [4]. The effect on induced velocity in the propeller plane is notable near the tip of the blade [11]. Tip-losses commonly refer to kinematic and/or dynamic differences between a two-dimensional and a three dimensional configuration of a lifting device. The main source of these differences for a wing of finite span or for a rotating propeller of finite number of blades is the circulation flow driven by the pressure equalization which arises at the tip of the lifting device [12]. Prandtl developed a correction and introduced it in the BET. The correction is highlighted below.

The tip correction parameter is calculated:

$$P_{tip(i,j)} = \frac{N_B(R_B - R_j)}{2R_j \cdot \sin\left(\varphi_{i,j} \cdot \frac{\pi}{180}\right)} \tag{29}$$

The tip factor is the determined:

$$F_{tip(i,j)} = \frac{2 \cdot \operatorname{acos}\left(e^{-P_{tip(i,j)}}\right)}{\pi} \tag{30}$$

The hub correction parameter is:

$$P_{hub(i,j)} = \frac{N_B(R_j - R_0)}{2R_j \cdot \sin\left(\varphi_{i,j} \cdot \frac{\pi}{180}\right)} \tag{31}$$

The hub correction factor is obtained:

$$F_{hub(i,j)} = \frac{2 \cdot \operatorname{acos}\left(e^{-P_{hub(i,j)}}\right)}{\pi} \tag{32}$$

After the determination of the tip and hub correction factors, the factor for the Prandtl correction is:

$$F_{tot(i,j)} = F_{tip(i,j)} \cdot F_{hub(i,j)} \tag{33}$$

The factor varies from 0 at the hub and tip, and close to 1 over the mid span and the blade [4].

3. VALIDATION CASE

For the validation of the mathematical modelling, blade element theory was implemented in a MATLAB program. The experiment was realized on a Caradonna-Tung rotor model. The Caradonna-Tung rotor has rectangular blades, without twist or sweep angles, and its section profile is a NACA 0012.

The aspect ratio of the rotor blade is 6, the chord length is 0.1905 m, and the rotor diameter is 2.286 m. The rotating speed is 1250 RPM and a tip Mach number of 0.439 as presented in [13].

The results obtained from the MATLAB program were compared with experimental data from [13]. It can be observed that both BET results and experimental data fit very well.

Fig. 5 presents the variation of thrust coefficient with collective pitch angle for both experimental data and BET results. Both data sets ensure a close alignment.

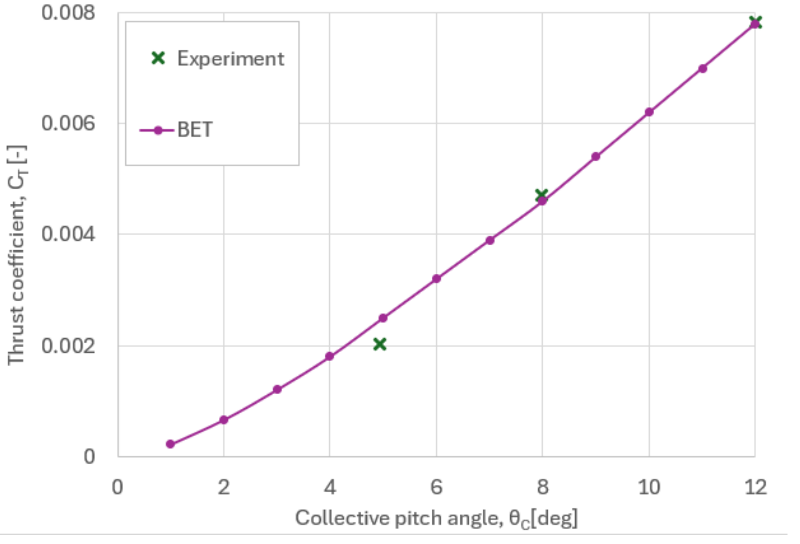

Fig. 5 Rotor thrust coefficient variation with collective pitch angle (Experimental data from [13] and BET results)

Fig. 6, Fig. 7, Fig. 8 highlight the variation of sectional thrust coefficient with radial station for collective pitch angles of 5˚, 8˚, respectively 12˚. For each variation, the radial section varies from 0, at the root of the rotor to 1, at the tip of the rotor.

The results obtained using BET method show that there are slight variations compared to experimental data and the Blade Element Theory can be used for the prediction of rotor thrust dependency.

Also, the difference between BET and experimental results are small and present only at the tip of the blade where the considered model for tip losses is not so accurate.

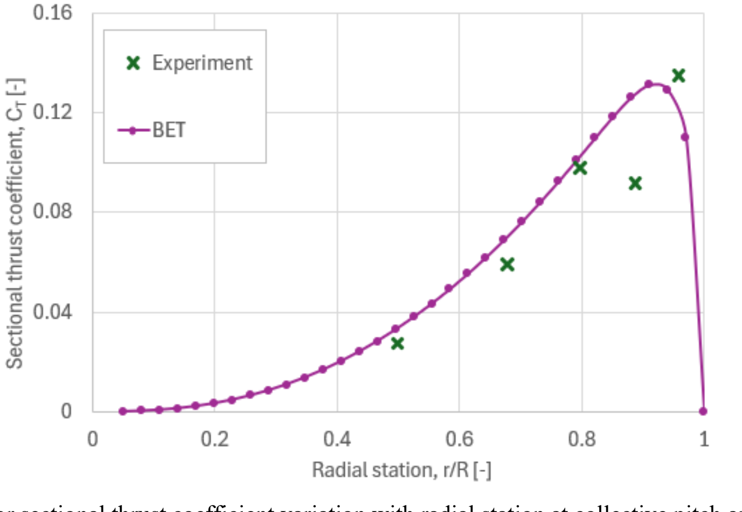

Fig. 6 Rotor sectional thrust coefficient variation with radial station at collective pitch angle of 5˚ (Experimental data from [13] and BET results)

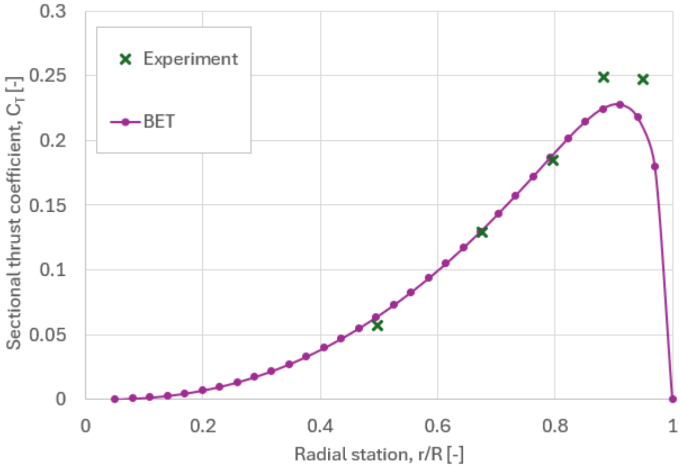

Fig. 7 Rotor sectional thrust coefficient variation with radial station at collective pitch angle of 8˚ (Experimental data from [13] and BET results)

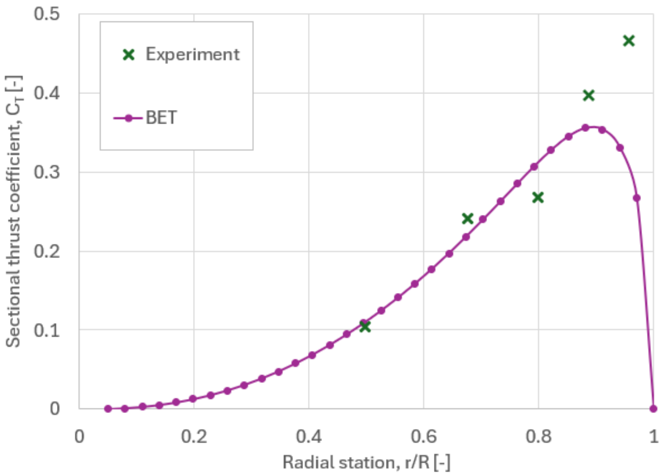

Fig. 8 Rotor sectional thrust coefficient variation with radial station at collective pitch angle of 12˚ (Experimental data from [13] and BET results)

4. STUDY CASE

A twin engine civil helicopter, with five seats configuration for transport, category A, three tone class and a four bladed main rotor was considered for the analysis. The rotor characteristics analyzed in the MATLAB program were: number of blades – 4, blade radius – 5.1 m, angular speed – 395 RPM and blade chord 0.3 m.

Two types of helicopter control were studied:

I. Collective pitch control – C = 5; A = 0; B = 0

II. Collective pitch with longitudinal cyclic pitch control – C = 5; A = 3; B = 0

The collective pitch control is used to make changes to the pitch angle of the main rotor blades and does this simultaneously, or collectively, as the name implies.

As the collective pitch control is raised, there is a simultaneous and equal increase in pitch angle of all main rotor blades; as it is lowered, there is a simultaneous and equal decrease in pitch angle [14].

The cyclic pitch control allows the pilot to fly the helicopter in any direction of travel: forward, rearward, left, and right.

The total lift force is always perpendicular to the tip-path plane of the main rotor. The purpose of the cyclic pitch control is to tilt the tip-path plane in the direction of the desired horizontal direction [14].

The prediction of rotor aerodynamics using blade element theory was performed using a MATLAB program. The program calculates the total thrust, resistive torque and power for the helicopter rotor performance.

Fig. 9, Fig. 10, Fig. 11 illustrate the variation of thrust, torque and power coefficients with the azimuth angle in order to evaluate the variation behaviour.

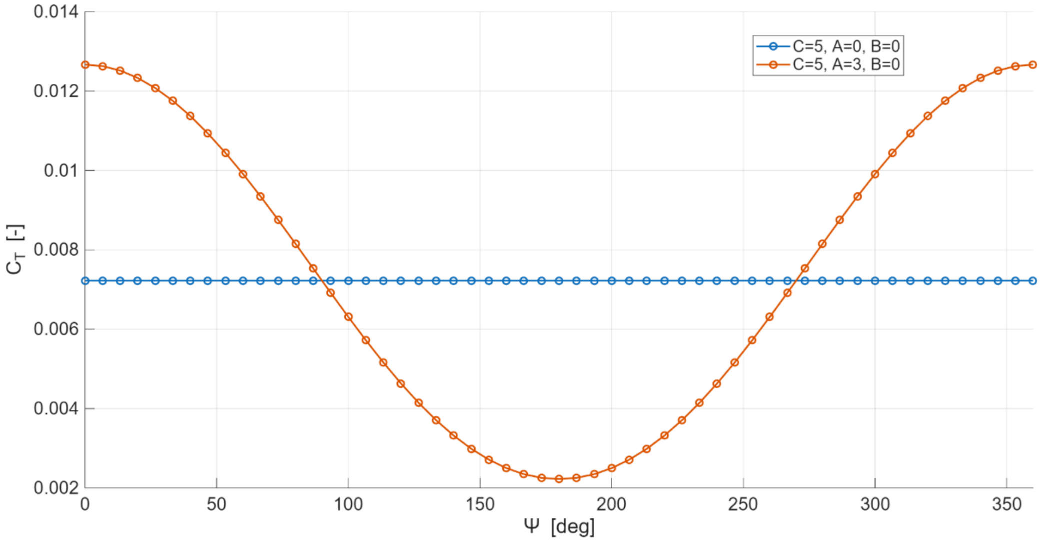

Fig. 9 Thrust coefficient variation with azimuth

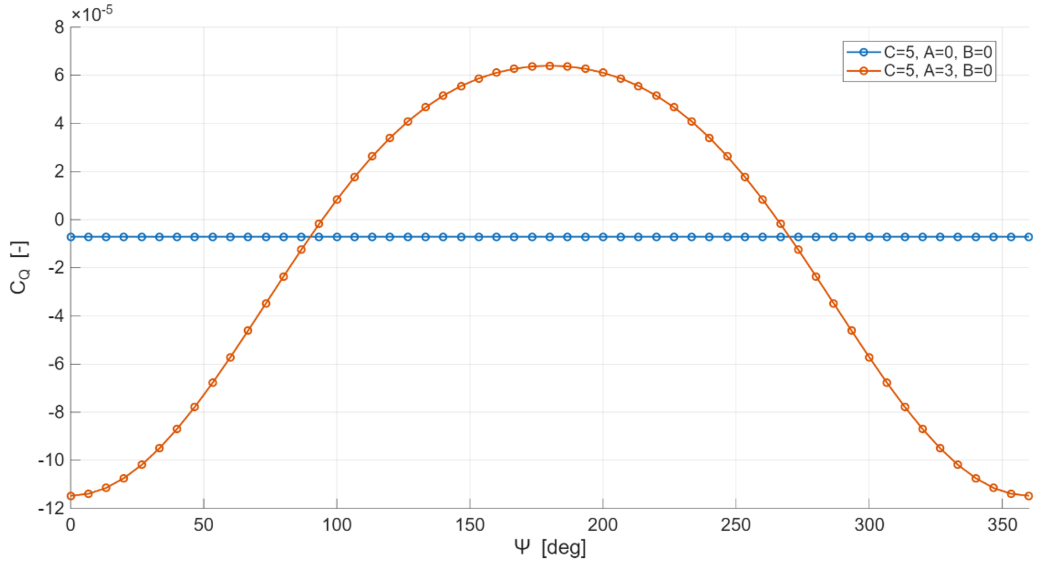

Fig. 10 Torque coefficient variation with azimuth

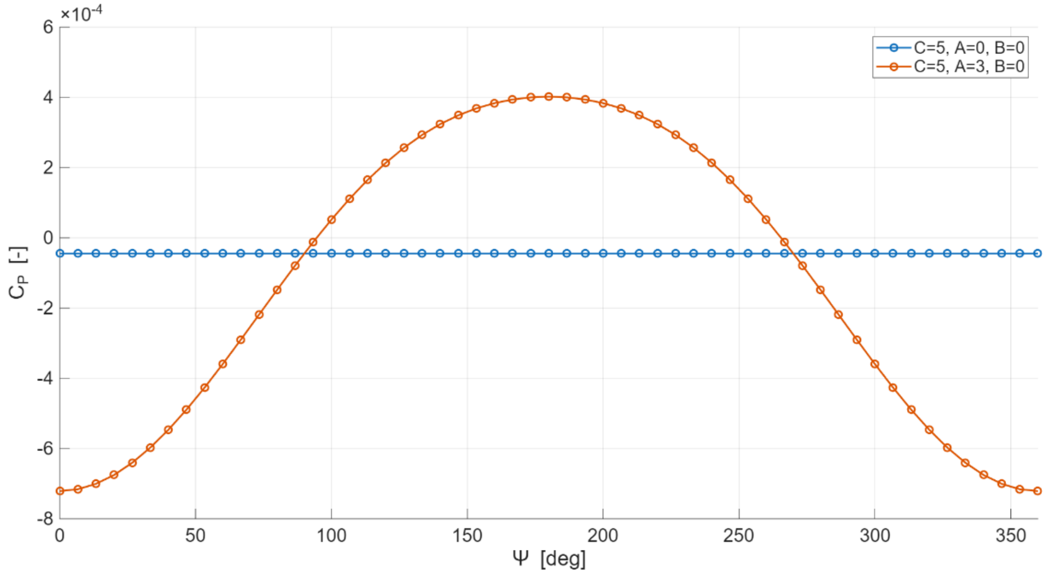

Fig. 11 Power coefficient variation with azimuth

The results obtained include the variation of the angle of incidence, of the induced velocity, of the elemental thrust, the elemental torque and of the elemental power for the two types of control considered.

Fig. 12 shows the variation of the angle of incidence in the rotor plane for both scenarios: collective pitch control only, and combined collective and cyclic pitch control.

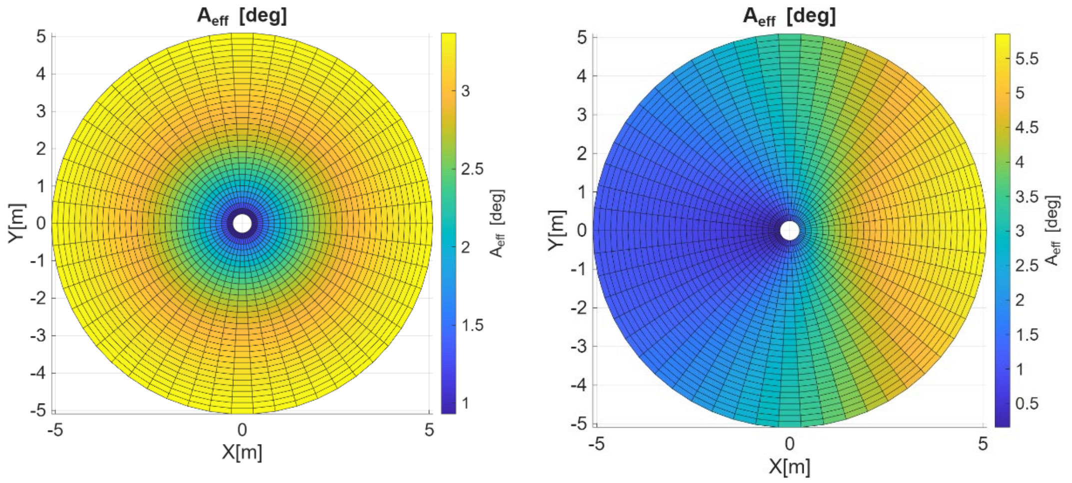

(a) (b)

Fig. 12 Angle of incidence variation for collective pitch control (a) and for collective pitch with longitudinal cyclic pitch control (b)

Fig. 13 shows the variation of the induced velocity in the rotor plane for both scenarios: collective pitch control only, and combined collective and cyclic pitch control.

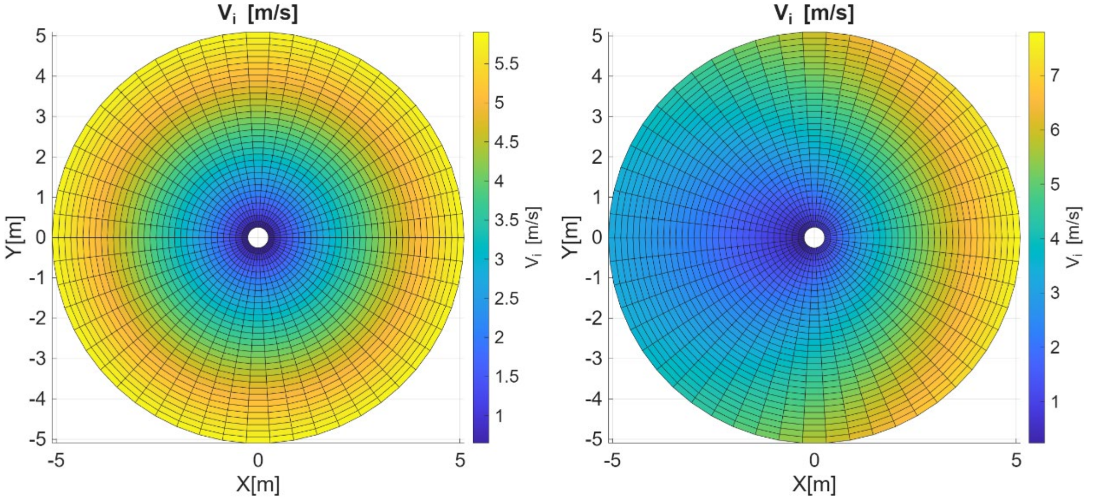

(a) (b)

Fig. 13 Induced velocity variation for collective pitch control (a) and for collective pitch with longitudinal cyclic pitch control (b)

Fig. 14 shows the variation of the elemental thrust in the rotor plane for both scenarios: collective pitch control only, and combined collective and cyclic pitch control.

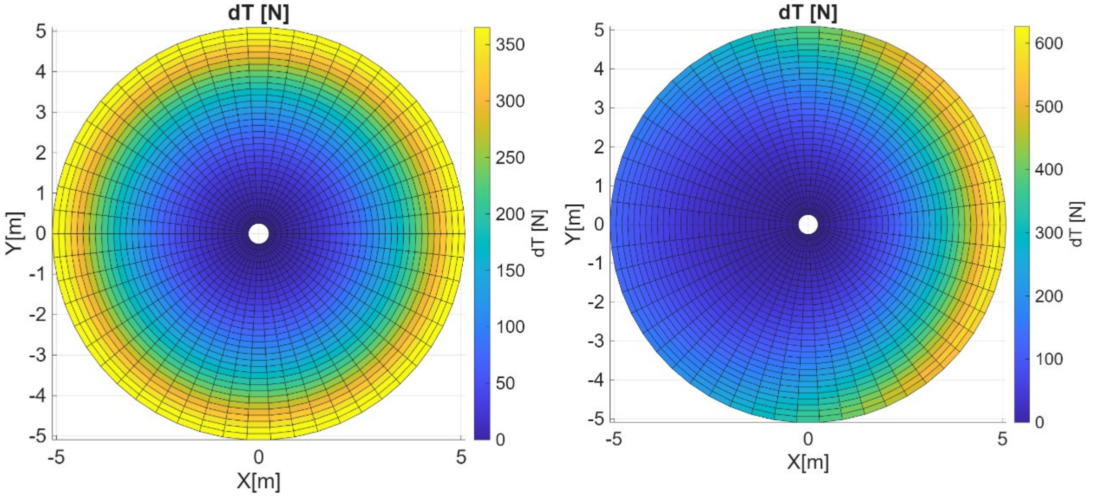

(a) (b)

Fig. 14 Elemental thrust variation for collective pitch control (a) and for collective pitch with longitudinal cyclic pitch control (b)

Fig. 15 shows the variation of the elemental torque in the rotor plane for both scenarios: collective pitch control only, and combined collective and cyclic pitch control.

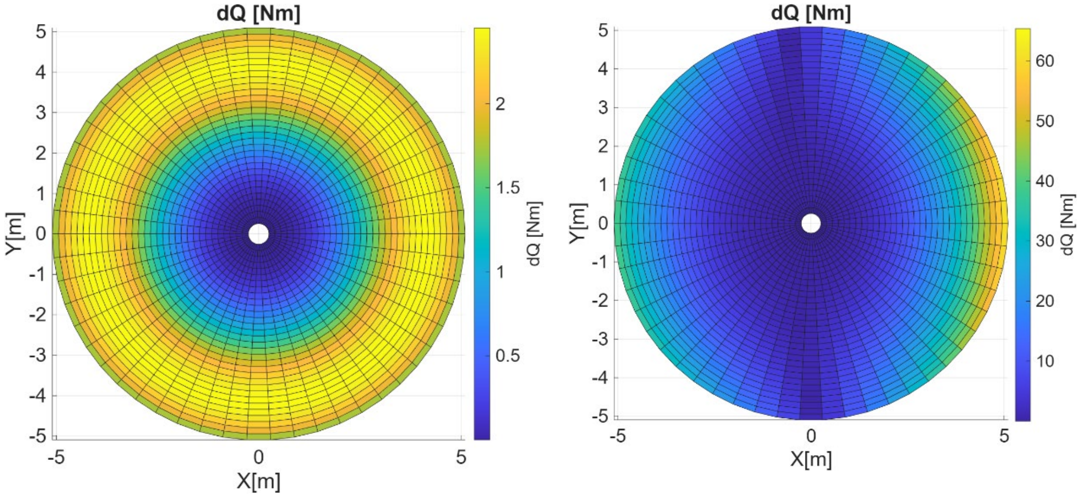

(a) (b)

Fig. 15 Elemental torque variation for collective pitch control (a) and for collective pitch with longitudinal cyclic pitch control (b)

Fig. 16 shows the variation of the elemental power in the rotor plane for both scenarios: collective pitch control only, and combined collective and cyclic pitch control.

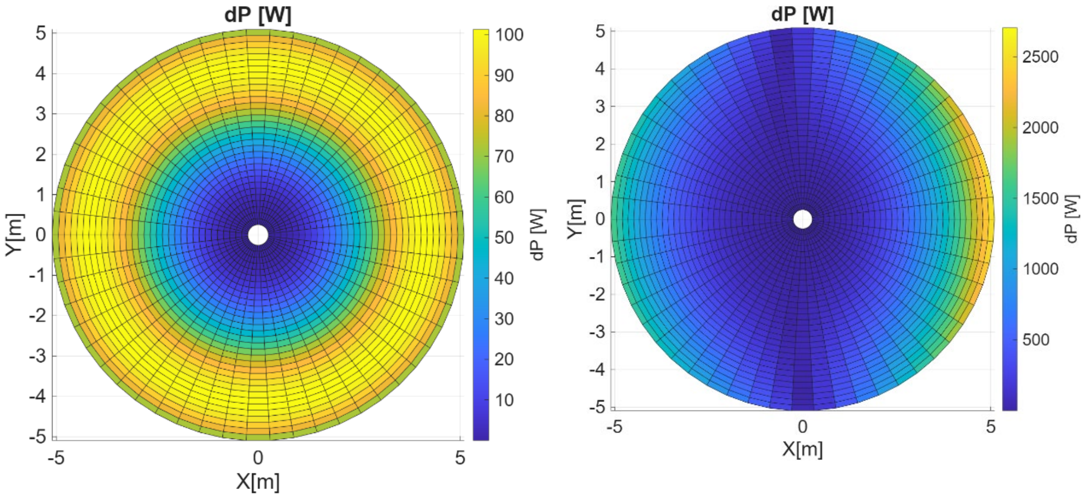

(a) (b)

Fig. 16 Elemental power variation for collective pitch control (a) and collective pitch with longitudinal cyclic pitch control (b)

5. CONCLUSIONS

The accurate estimation of aerodynamic coefficient is essential for predicting thrust, torque, and power using Blade Element Theory (BET) and for optimizing rotorcraft performance. The comparison between the MATLAB implementation and experimental data demonstrates that BET provides reliable results while enabling rapid parametric studies of pitch settings and blade geometry. Owing to its low computational cost, the developed BET code is well suited for integration into rotorcraft optimization frameworks and helicopter flight dynamics models.

BET captures the primary dependencies of rotor thrust, torque, and power on collective and cyclic pitch, rotational speed, and blade geometry. The method is based on the assumption of rigid blades, neglecting aeroelastic effects, and requires hub and tip-loss corrections to account for reduced lift, particularly at high angles of attack.

The validation case shows good agreement with experimental measurements, with the main discrepancies occurring near the blade tip, where the employed tip-loss model presents limited accuracy.

The study conducted on a representative rotor demonstrates that BET enables efficient investigation of operational parameters (collective and cyclic pitch, forward and climb speed, rotor incidence) as well as geometric parameters (blade planform and airfoil selection). Although the present implementation is limited to constant chord and linear twist distributions, it can be extended to account for nonlinear distributions to support more advanced geometry optimization.

Overall, BET offers an effective balance between accuracy and computational efficiency for rapid aerodynamic performance evaluation of rotary-wing systems, including helicopter rotors, propellers, and wind turbines. The agreement with experimental data confirms the validity of both the method and the developed program, supporting their use in future design, optimization, and flight-dynamics studies.

REFERENCES

[1] R. H. Miller, "The Aerodynamics and Dynamics of Rotors - Problems and Perspectives," in *C.A. (eds) Recent Advances in Aerodynamics. Springer*, New York, 1986.

[2] S. Drzewiecki, *Théorie générale de l'hélice: hélice aériennes et hélices marines*, University of Michigan Library, 1920.

[3] K. E. Schoenherr, *Resistance of flat surfaces moving through a fluid,* Trans. Soc. Nav. Arch. Mar. Eng., 1932.

[4] S. Gudmundsson, "Thrust Modeling for Propellers," in *General Aviation Aircraft Design*, Butterworth-Heinemann, 2022, pp. 646-656.

[5] J. Gordon Leishman, *Principles of Helicopter Aerodynamics*, Cambridge University Press, 2000.

[6] J. Seddon, *Basic Helicopter Aeodynamics*, British Library, 1990.

[7] W. Z. Stepniewski, "Rotary-*Wing Aerodynamics. Volume I - Basic Theories of Rotor Aerodynamics (With Application to Helicopters)*," NASA, Philadelphia, 1979.

[8] W. Johnson, *Helicopter Theory*, Dover Publications, 1980.

[9] M. Tai, W. Lee, D. Kim and D. Park, "Improvements in Robustness and Versatility of Blade Element Momentum Theory for UAM/AAM Applications," *Aerospace,* vol. **8**, no. 12, p. 728, 2025.

[10] S. Gudmundsson, "Thrust Modelling for Propellers," in *General Aviation Aircraft Design*, Butterworth-Heinemann, 2022, pp. 638-645.

[11] M. K. Rwigema, "Propeller blade element momentum theory with vortex wake deflection," in *27TH INTERNATIONAL CONGRESS OF THE AERONAUTICAL SCIENCES.*

[12] E. Branlard and M. Gaunaa, "Development of new tip-loss corrections based on vortex theory and vortex methods," *Journal of Physics Conference Series,* vol. **555**, no. 1, 2014.

[13] F. X. Caradonna and T. C., "Experimental and Analytical Studies of a Model Helicopter Rotor in Hover," in *European Rotorcraft and Powered Lift Aircraft Forum*, 1981.

[14] * * * U.S. Department of Transportation, Helicopter Flying Handbook, Federal Aviation Administration, 2019.